# Observation of the Transfer of the Local Angular Momentum Density of a Multiringed Light Beam to an Optically Trapped Particle

V. Garcés-Chávez,[1,*] D. McGloin,[1] M. J. Padgett,[2] W. Dultz,[3] H. Schmitzer,[4] and K. Dholakia[1]

[1]*School of Physics and Astronomy, University of St. Andrews, North Haugh, St. Andrews, KY16 9SS, United Kingdom*
[2]*Department of Physics and Astronomy, Kelvin Building, University of Glasgow, Glasgow G12 8QQ, United Kingdom*
[3]*Johann Wolfgang Goethe-Universitat, Phyikalisches Institut (Fb 13), Robert Mayer Strasse 2-4 D-60054 Frankfurt am Main, Germany*
[4]*Department of Physics, Xavier University, 3800 Victory Parkway, Cincinnati, Ohio 45207, USA*

(Received 20 December 2002; published 29 August 2003)

We observe the spinning and orbital motion of a microscopic particle trapped within a multiringed light beam that arises from the transfer of the spin and orbital components of the light's angular momentum. The two rotation rates are measured as a function of the distance between the particle and the axis of the trapping beam. The radial dependence of these observations is found to be in close agreement with the accepted theory.

DOI: 10.1103/PhysRevLett.91.093602 PACS numbers: 42.50.Vk, 41.85.–p, 42.50.Ct, 87.80.Cc

Optical tweezers have been used by a number of groups to investigate the transfer of both spin and orbital angular momentum (OAM) to trapped microscopic particles. The first observation was of the transfer of orbital angular momentum to an absorbing particle trapped on the beam axis thereby causing it to rotate [1]. Subsequently, the same group observed the transfer of spin angular momentum (SAM) [2]. In that experiment, a birefringent particle acted as a tiny half-wave plate and was set spinning by a circularly polarized trapping beam: effectively a microscopic version of Beth's classic experiment of the 1930s [3]. Two early tweezing experiments involving both the spin and orbital angular momentum used absorbing particles and observed the speeding up or slowing down of the rotation rate as the spin and orbital components were added or subtracted [4,5].

However, restricting the interaction to particles held on the beam axis does not enable the intrinsic or extrinsic nature of the angular momentum to be explored — for this, the interaction needs to be with particles held away from the beam axis. In principle, the spin angular momentum should cause a particle to spin about its own axis, whereas the orbital angular momentum should cause the particle to orbit around the beam axis. Again optical tweezers can be used, taking advantage of the annular form of the Laguerre-Gaussian or Bessel modes so that a particle may naturally be confined to a region away from the beam axis. The first observation of a particle "orbiting" around the beam axis was related to the scattering of light by, and the subsequent motion of, metallic particles [6]. More regular orbital motion has also been observed for high and low index transparent particles trapped in various rings of a Bessel beam [7,8]. The first experiment to observe particles displaced from the beam axis spinning both about their own axis and separately about the beam axis used a circularly polarized Laguerre-Gaussian mode acting on birefringent and scattering particles, respectively [9].

Generally, the experimental uncertainties within all these tweezing experiments make quantitative comparison between observed and predicted rotation rates impossible. In this Letter, we report the first quantitative measurements simultaneously relating the spin and orbital angular momentum content of a light beam acting on a single particle held off axis. For a particle trapped away from the beam axis, no such comparisons have yet been made since the spinning and orbiting have only been observed on different particle types at a fixed radius. This we achieve by observing both the spinning and orbiting of the same particle trapped at various distances from the beam axis in a multiringed Bessel beam. It is then possible to make measurements that can be compared directly to the theoretical predictions.

The linear momentum density of any arbitrary beam can be calculated directly from the complex amplitude of the electromagnetic field, $u \equiv u(r, \phi, z)$, where $r$, $\phi$, and $z$ are the radial, azimuthal, and longitudinal coordinates, respectively. Within the paraxial approximation, this is given by [10]

$$\begin{aligned}\mathbf{p} &= \varepsilon_0/2(\mathbf{E}^* \times \mathbf{B} + \mathbf{E} \times \mathbf{B}^*) \\ &= i\omega\frac{\varepsilon_0}{2}(u^*\nabla u - u\nabla u^*) + \omega k\varepsilon_0|u|^2\hat{\mathbf{z}} \\ &\quad + \omega\sigma\frac{\varepsilon_0}{2}\frac{\partial|u|^2}{\partial r}\hat{\boldsymbol{\phi}}, \end{aligned} \tag{1}$$

where $\hat{\mathbf{z}}$ and $\hat{\boldsymbol{\phi}}$ are unit vectors and $\sigma$ is the degree of polarization of the light; $\sigma = \pm 1$ for right- and left-hand circularly polarized light, respectively, $\omega$ is the angular frequency of the light, $k$ the wave vector of the light, and the other symbols have their usual meaning.

The angular momentum density in the $z$ direction depends upon the $\phi$ component of $\mathbf{p}$, such that $j_z = rp_\phi$. The third terms of Eq. (1) are associated with the spin angular momentum. As reasoned by Simmons and Guttmann [11], despite the dependence of this term on

  

the intensity gradient the spin angular momentum component is always $\sigma\hbar$ per photon when integrated across the beam profile. Hence, a quarter-wave plate, suspended in a much larger circularly polarized beam, will experience a torque about the axis of the wave plate not the axis of the beam. The absolute magnitude of this torque depends upon the details of the transfer mechanism. For complete absorption of the light by the particle, the torque corresponds to an angular momentum of $\sigma\hbar$ per photon. For a birefringent particle, the torque depends on to what extent the thickness and birefringence of the material changes the polarization state of the beam. However, for any particular particle, the torque is simply proportional to the local intensity of the beam. Thus, the spin rotation rate of a single particle effectively acts to serve as a local measure of the beam intensity and of the spin angular momentum of the beam.

As is now well documented, the orbital angular momentum is related to the azimuthal phase gradient of the field and can be linked directly to the first term of Eq. (1). It arises from the azimuthal component of the momentum vector. For beams with helical phasefronts, such as Laguerre-Gaussian or high-order Bessel beams, the complex field amplitude, in units of the vector potential, can be written as [10] $u(r, \phi, z) = u(r, z)\exp(il\phi)$. For a circularly polarized beam propagating in the $z$ direction, the $r$, $\phi$, and $z$ components of the linear momentum density are given by [12]

$$p_r = \epsilon_0 \frac{\omega k r z}{(z_R^2 + z^2)}|u|^2,$$
$$p_\phi = \epsilon_0\left[\frac{\omega l}{r}|u|^2 - \frac{1}{2}\omega\sigma\frac{\partial|u|^2}{\partial r}\right], \quad (2)$$
$$p_z = \epsilon_0\omega k|u|^2.$$

These can be alternatively expressed in terms of the momentum contribution per photon:

$$p_r = \frac{\hbar k r z}{(z_R^2 + z^2)},$$
$$p_\phi = \left[\frac{l\hbar}{r} - \frac{\hbar}{2|u|^2}\sigma\frac{\partial|u|^2}{\partial r}\right], \quad (3)$$
$$p_z = \hbar k,$$

where $z_R$ is the Rayleigh range of the beam.

Again, the orbital ($l$) and spin ($\sigma$) contributions to the angular momentum can be clearly identified and separated. When the orbital term is integrated over the whole beam, this gives an angular momentum of $l\hbar$ per photon. However, as discussed in [9] for a small particle held in a much larger beam, the total angular momentum is not relevant; instead the interaction should be considered purely in terms of the azimuthal component of the linear momentum density which, from Eq. (3), we see is $l\hbar/r$ per photon. It is this term that is responsible for the orbital motion of the trapped particles reported in Refs. [7,9]. For any given particle, the force is proportional to the azimuthal mode index, to the local intensity, and inversely proportional to the radius away from the beam axis. As with the spinning motion, the absolute magnitude of this azimuthal force depends on the details of the transfer mechanism. For complete absorption of the light by the particle, the force corresponds to a linear momentum of $l\hbar/r$ per photon. For nonabsorbing particles, the torque depends upon the degree to which the incident light is scattered.

We made use of our standard geometry high-order $J_2$ Bessel beam (HOBB) tweezers setup [13] operating at 1064 nm to study the particle motion produced by the transfer of either OAM or SAM to a confined fragment of mercury chloride (kalomel). The Bessel beam was generated using an axicon illuminated with a $l = 2$ Laguerre-Gaussian (LG) beam and had an inner ring radius of 2.9 $\mu$m. The HOBB was circularly polarized by inserting a quarter-wave plate in the system. The experimental sample consisted of birefringent mercury chloride particles suspended in $D_2O$ plus a small quantity of detergent. We placed 20 $\mu$l of this solution between two coverslips separated by a spacer of about 100 $\mu$m thickness. The sample was placed in an $xyz$ translation stage for full control of the position of the sample. A small birefringent particle was chosen as our probe particle. In Fig. 1, we can see the motion of a trapped fragment of mercury chloride. The particle was seen to rotate around its own axis (due to SAM) and also traverse the beam

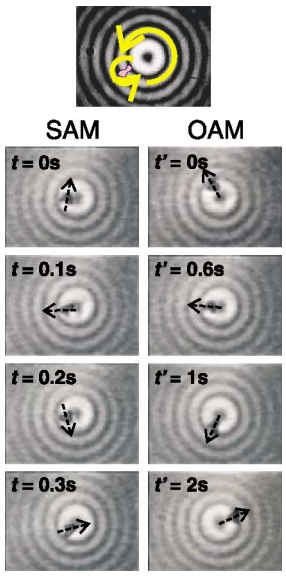


FIG. 1 (color online). A birefringent particle trapped in the first ring of a HOBB rotates simultaneously (i) around its own axis (due to SAM) and (ii) around the beam's axis (due to OAM). The frames were taken from a video at the time indicated in each box.

circumference due to OAM [14]. Changing the handedness of the polarization changed the rotation sense about the particle axis but not the sense of rotation around the beam axis. Inserting a Dove prism in the system causes the particles to traverse the beam circumference in the opposite sense.

When considering the motion of small particles within a much larger, circular polarized multiringed beam with helical wave fronts, a number of predictions can be made. To a first approximation, the energy contained in each of the rings of the Bessel beam is equal [15], giving a local intensity inversely proportional to the ring radius. It follows that, for a particular birefringent or absorbing particle, the transfer of a light beam's spin angular momentum leads to a spin rate of the particle about its own axis ($\Omega_{\text{spin}}$) inversely proportional to the radius of the ring in which it is trapped, i.e.,

$$\Omega_{\text{spin}} \propto \sigma/r. \tag{4}$$

By contrast for a specific absorbing or scattering particle, the transfer of the orbital angular momentum leads to an azimuthal force that is inversely proportional to the square of the radius of the ring in which it is trapped. This leads to an orbital rotation rate ($\Omega_{\text{orbit}}$) inversely proportional to the cube of the ring radius:

$$\Omega_{\text{orbit}} \propto l/r^3. \tag{5}$$

Since the absolute rotation rates depend upon detailed parameters beyond experimental control, the predictions made by Eqs. (4) and (5) can be verified only by measuring the spin and orbital motion of the same particle at various radii from the beam axis. For a birefringent particle small enough to also react to the scattering force, its spin and orbital motion should be observable simultaneously.

In our experiment, by moving the sample stage, we could place our probe birefringent particle in each one of the first five rings of the HOBB. In order to measure the spin and orbital rotation rates, a sequence of frames was recorded. The rotation of the same particle of 1 $\mu$m width and 3 $\mu$m length was obtained for different values of the radius ($r$) of the beam. We repeated the experiment for different values of laser power. Figure 2 shows the results obtained after taking an average of several measurements in each experiment. Each set of data points relates to a single trapped particle. As predicted, the rotation rates due to the spin have a linear dependence on the power and decrease as $1/r$ for the same power. For the case of the rotation rates due to the orbital angular momentum, we also found a linear dependence on the power but now the rotation rates are proportional to $1/r^3$, as predicted. This may be deemed an actual measurement of both the local intensity and importantly local angular momentum density of the light beam *in situ*.

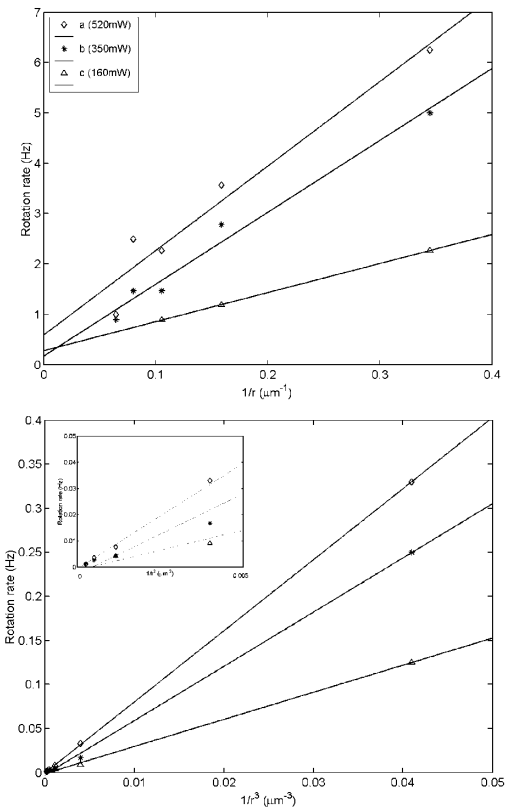


FIG. 2. Spin and orbital rotation rate as a function of $1/r$ (top) and $1/r^3$ (bottom) for different beam powers, denoted by ($\diamond$) 520 mW, (*) 350 mW, and ($\triangle$) 160 mW. Here $r$ is the distance away from the beam's optical axis. The data is for a $1 \times 3$ $\mu$m particle. The inset in the lower graph shows an expansion of the scale close to the origin.

We also implemented a novel method to measure the local AM density in any part of a light beam (proposed in [16]). By monitoring the temporal intensity variation of the transmitted light through our partially transparent probe particle, we could measure the spin and orbital rotation rates, respectively, of the particle. When the light passes through a birefringent particle, the light changes its polarization [2]. By measuring the power before and after passage through the trapped birefringent particle, one may measure the polarization change of the circularly polarized light due to the particle [16]. The rotation rate was then derived from the period of the signal variation. In order to observe the transfer of local AM density from the beam, we placed a pinhole in the path of the transmitted light beam. The light traversing the pinhole is sent to a photodiode.

In this instance, we used a circularly polarized LG beam $l = 2$ focused to 50 $\mu$m to observe the simultaneous local transfer of SAM and OAM to our probe particle. The reflected light is sent to a charge-coupled device camera in order to see the trapped particle. The

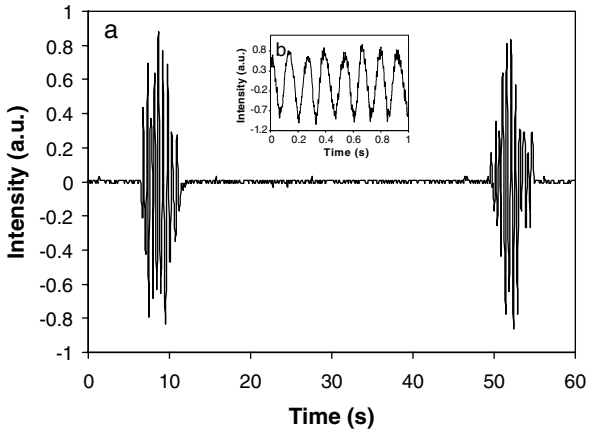


FIG. 3. Detected signals from a rotating birefringent microscopic particle in a LG beam. Trace (a) indicates the orbital motion of the particle around the beam axis, as the particle passes in front of the pinhole, with the period calculated from the time between each large oscillation region ($\sim 0.02$ Hz). Trace (b) shows a snapshot of one of the large oscillation regions and indicates the rotation rate due to SAM ($\sim 5$ Hz).

transmitted beam is collected by $\times 60$ microscope objective. The mean power measured through the polarizer is half of the power incident of the particle. The frequency of the variation is twice the rotation rate of the particle. The signal collected by the photodiode is shown in Fig. 3 for a specific location of the pinhole. In this figure, we show two different traces. Each time that the particle passes over the pinhole, the photodiode records a signal, shown in Fig. 3(a). Therefore, we can measure the rotation of the probe particle due to the orbital AM by the trace signal and at the same time we can see the rotation due to the SAM [Fig. 3(b)]. We have noticed that when the particle is highly asymmetrical the sinusoidal nature of the recorded trace due to the spin rotation is perturbed and becomes more complicated, with a number of frequency components present. For any kind of light beam, we can use this method to record the local AM in any part of the beam.

In conclusion, we have demonstrated experimentally the transfer of spin and orbital angular momentum to an off-axis particle. We have used a birefringent particle as a probe of the optical field and studied the local angular momentum density of a multiringed light beam, finding a good agreement with theory. A new technique to determine the instantaneous rate of rotation due to SAM and the orbiting rate due to OAM has also been presented.

This work was funded by the Leverhulme Trust and the EPSRC. M. J. P. acknowledges support from the Royal Society.

*Corresponding author.
Electronic address: gv3@st-and.ac.uk

[1] H. He, M. E. J. Friese, N. R. Heckenberg, and H. Rubinsztein-Dunlop, Phys. Rev. Lett. **75** , 826 (1995).
[2] M. E. J. Friese, T. A. Niemenen, N. R. Heckenberg, and H. Rubinsztein-Dunlop, Nature (London) **394**, 348 (1998).
[3] R. A. Beth, Phys. Rev. **50**, 115 (1936).
[4] M. E. J. Friese, J. Enger, H. Rubinsztein-Dunlop, and N. R. Heckenberg, Phys. Rev. A **54**, 1593 (1996).
[5] N. B. Simpson, K. Dholakia, L. Allen, and M. J. Padgett, Opt. Lett. **22**, 52 (1997).
[6] A. T. O'Neil and M. J. Padgett, Opt. Commun. **185**, 139 (2000).
[7] K. Volke-Sepulveda, V. Garcés-Chávez, S. Chávez-Cerda, J. Arlt, and K. Dholakia, J. Opt. B **4**, S82 (2002).
[8] V. Garcés-Chávez, K. Volke-Sepulveda, S. Chávez-Cerda, W. Sibbett, and K. Dholakia, Phys. Rev. A **66**, 063402 (2002).
[9] A. T. O'Neil, I. MacVicar, L. Allen, and M. J. Padgett, Phys. Rev. Lett. **88**, 053601 (2002).
[10] L. Allen, M. W. Beijersbergen, R. J. C. Spreeuw, and J. P. Woerdman, Phys. Rev. A **45**, 8185 (1992).
[11] J. W. Simmons and M. J. Guttmann, *States, Waves and Photons* (Addison-Wesley, Reading, MA, 1970).
[12] L. Allen and M. J. Padgett, Opt. Commun. **184**, 67 (2000).
[13] J. Arlt, V. Garcés-Chávez, W. Sibbett, and K. Dholakia, Opt. Commun. **197**, 239 (2001).
[14] See EPAPS Document No. E-PRLTAO-91-030334 for a video showing the rotation of a mercury chloride particle in the first ring of a high-order Bessel beam. The particle is clearly seen to rotate both about its own axis (due to SAM) and the beam (due to OAM) axis. A direct link to this document may be found in the online article's HTML reference section. The document may also be reached via the EPAPS homepage (http://www.aip.org/pubservs/epaps.html) or from ftp.aip.org in the directory /epaps/. See the EPAPS homepage for more information.
[15] J. Durnin, J. Opt. Soc. Am. A **4**, 651 (1987).
[16] T. A. Nieminen, N. R. Heckenberg, and Rubinsztein-Dunlop, J. Mod. Opt. **48**, 405 (2001).